PAPER

Check for updates

In-line monitoring of resorcinol–formaldehyde gelation using fiber optic UV-vis spectroscopy in real time: part I†

Seeni Meera Kamal Mohamed, [ID] * Kavita Möllmann, Charlotte Heinrich, [ID] Marina Schwan [ID] and Barbara Milow

The sol–gel transition of resorcinol–formaldehyde (RF) solutions in the presence of sodium carbonate as a catalyst was monitored using in-line UV-vis measurements in real time by observing the absorbance changes at various gelation temperatures using a fiber-optic probe. The two absorbance maxima at around 340–400 and 500 nm were caused by different resorcinol derivatives and *O*-quinone methide intermediates, respectively, which were formed during the gelation. The absorbance was measured until visible turbidity appeared. The turbidity time (t_{turb}) was determined, and it was found to decrease with increasing gelation temperatures. The general absorbance behaviour and the trend in absorbance value variations in correlation with time and at three different wavelengths (460, 485 and 510 nm) were studied for different gelation temperatures, and the observed correlation was presented and discussed for each temperature. The research method developed in this investigation helps in understanding and optimizing the synthesis process of RF aerogels on a laboratory scale. A simple transfer to process monitoring in industrial production seems possible.

1. Introduction

Resorcinol–formaldehyde (RF) aerogels have been studied extensively since their discovery by Pekala *et al.*[1] RF aerogels have high surface areas and porosities and low densities, making them applicable in the field of thermal and acoustic insulation.[2–4] They are the most common initial materials for the preparation of carbon aerogels, which involves their pyrolysis under inert conditions. Carbon aerogels are a unique class of porous materials that exhibit high porosities (90–98 vol%), high surface areas, low thermal conductivities, and high electrical conductivities, which make them suitable for different applications, including in adsorbents and foundries, electrochemical devices (double-layer supercapacitors, batteries, and fuel cells), gas storage, catalysis and gas separation.[2–4] The widely accepted mechanism for the RF reaction proceeds through an initial addition between R and F followed by self-condensation of oligomeric chains to form colloidal particles and a 3D-gel network.[5] Several parameters in the sol–gel process influence the porosity, morphology and total solid content of RF aerogels, which include initial pH of the RF solution, R/F molar ratio, R-to-catalyst (C) (R/C) ratio (includes type and concentration of the catalyst), R-to-water (W) (R/W) ratio, dilution ratio (D), *i.e.*, D = W/(R + F + C), methanol content in formaldehyde, gelation temperatures and drying methods.[6–8] There are two main mechanisms reported for the formation and control of networks in RF aerogels: (i) microphase separation and (ii) aggregation of primary colloidal particles to form different 3D-gel network structures.[9–11] The investigations on the mechanism of RF gel formation (physical or chemical) and the kinetics of the reactions between R and F are limited to certain studies because in most cases, the mechanism suggested by Pekala is assumed and validated.[12] There are only a limited number of studies reported in the literature on the kinetic monitoring of early stages of RF gel formation using different physico-chemical and microscopic techniques such as dynamic light scattering (DLS),[10] small-angle X-ray scattering (SAXS),[13] scanning electron microscopy (SEM),[9] transmission electron microscopy (TEM),[9] nuclear magnetic resonance (NMR),[14,15] infra-red (FT-IR) spectroscopy and Raman spectroscopy.[16,17]

In general, RF aerogels are dark red to purple or brown (dark or light) in color depending upon the initial pH of the RF solution.[18] UV-vis characteristic red color transition of the HCl-catalysed RF solution in acetonitrile is observed at 543 nm, due to the formation of reactive and unstable *O*-quinone methide as an intermediate similar to the base-catalysed reaction between phenol and formaldehyde (PF).[19] It requires a few minutes to build up red color in acid catalysts, whereas it requires a few

Department of Aerogels and Aerogel Composites, Institute of Materials Research, German Aerospace Center (DLR), Cologne, Germany. E-mail: seenimeera. kamalmohamed@dlr.de

hours to several days in case of base-catalysed reactions.[19] These unstable *O*-quinone methide intermediates further react with resorcinol to form stable methylene (–CH$_2$) bridged structures.[20] The simultaneous development of color and buildup of the viscosity of the RF solution leads to gelation and results in different colored aerogel monoliths. The appearance of different colors in the aerogel monoliths is related to the configurational locking of quinone and/or spiro derivatives.[21] Hence, an extensive investigation dedicated to the monitoring of the early-stage kinetics of the reaction between R and F by observing the absorbance changes using in-line ultra-violet visible (UV-vis) spectroscopy in real time is inevitable.

However, limited numbers of studies have been published on the UV-vis investigation of early-stage reactions between R and F. In 1936, Engeldinger[22] reported on a spectrophotometric approach for investigating the kinetics of phenolic condensation by measuring the light absorption at 490 nm during the reaction of R with F. Later, Stedry[23] studied reaction rates of a mixture of R and F at temperatures from 286 to 316 K. The most prominent transmittance changes were observed in the wavelengths ranging from 300 to 400 nm with respect to reaction time and temperature. It has been observed that transmittance becomes weaker in the wavelength range of 300 and 500 nm.[23] Further, a peak at 245 nm shifted to higher wavelengths with the decrease in intensity in the course of the reaction.[23] In recent years, UV-vis spectroscopy used to monitor the reaction progress of RF gelation over the range of 200–800 nm with various metal carbonate catalysts.[24]

In comparison to other techniques, it is easy to set up UV-vis measurements and interpret the results. The short integration time in the millisecond range provides rapid results with high sensitivity. The current study employs the use of in-line measurements using a fiber-optic immersion probe in real time. In-line UV-vis spectroscopy was used to study the dynamics of cleaning in place of membrane filtration in whey filtration plants,[25] monitoring of continuous hot melt extrusion manufacturing process,[26] membrane fouling dynamics in the low-filtration process,[27] dissolution of the Al–Zn–Mg–Cu alloy in a HCl solution,[28] to find the concentration of hydroxyl radicals formed during UV photolysis of hydrogen peroxide,[29] monitor the metal–ligand exchange process,[30] and further more. Hence, the investigation and monitoring of early stages of RF gelation kinetics play crucial roles in understanding the physicochemical changes occurring during the sol–gel process. This will enable researchers to understand, optimize and quantify the process time, energy consumption, chemical requirements, mechanism, chemical species involved, and thus costs of aerogel production.

In the current investigation, the monitoring of RF gelation using a fiber-optic probe enabled UV-vis-Near Infra-red (UV-vis-NIR) spectroscopy to be performed at different temperatures. The molar ratios of the RF reactants were fixed as R/F 0.74, R/C 1500 and R/W 0.044. The initial pH of RF was measured between 6.0 and 6.15 using a constant volume of mixtures throughout the study. The gelation temperatures were varied from room temperature to higher temperatures until 80 °C and the absorbance changes were observed until permanent

turbidity appeared. The main focus of this study is to understand the absorbance changes appearing during the gelation process with respect to two peaks at around 340 and 510 nm.

2. Experimental section

2.1. Materials

Resorcinol (solid, 98%) and sodium carbonate (solid, anhydrous, 99.8%) were purchased from Sigma-Aldrich, Germany. 23.5% formaldehyde, low concentrated methanol solutions were procured from Carl Roth, Germany. Ethanol (99.9%) was obtained from Th. Geyer, Germany for solvent exchange and super-critical drying. Deionized water was used throughout the experiments. All the reagents were used as received without further purification.

2.2. Preparation of RF solution

RF solution was prepared by mixing the following reactants: resorcinol, 23.5% formaldehyde, water and sodium carbonate. The ratios of R/C, R/F and R/W were used as 1500, 0.74 and 0.044, respectively. First, resorcinol was mixed with water under stirring for 10 minutes, and then a required amount of formaldehyde was added and stirred for another 10 minutes. Afterwards, the calculated amount of sodium carbonate catalyst was added and stirred continuously for 40 minutes until the pH of the solution was constant. The initial pH of the RF solution was observed between 6.0 and 6.15 before placing the reaction container at elevated temperatures inside the oven. Moreover, we did not monitor the pH change during the gelation process at elevated temperatures.

2.3. Instrument parameters

The monitoring of RF reaction was studied using an in-line optical fiber probe (Hellma GmbH & Co. KG, Germany) connected to a UV-vis spectrometer (MultiSpec®UV-NIR from tec 5 AG, Germany). The measurement scans covered a wavelength range of 190–1100 nm, with a path length of 10 mm and a resolution set at 1 nm.

2.4. Data analysis and graph processing

The plotting, smoothing and connections (B-spline) of the data point were performed using the Origin 2019b (version 9.6.5.169) software. Some of the data points were skipped to achieve good shape of the graph during the graph processing stage. The shifting of the first absorbance maximum value in the wavelength region of 340–400 nm and the second absorbance maximum value at three different wavelengths (460, 480 and 510 nm) were extracted automatically using the Origin software with different commands.

2.5. In-line UV-vis spectroscopy measurements

The UV-vis spectra of the reaction mixture were recorded at every step of reactant addition followed by 10 minutes of stirring. After measuring the initial pH of the RF solution, the UV-vis spectra were recorded again. Then, the RF solution was

Fig. 1 Experimental set-up for conducting in-line UV-vis measurements in real time.

Fig. 3 Plot of turbidity time *versus* gelation temperature (inset: transition from brownish red color to turbid formation).

placed inside a pre-heated oven at different temperatures, namely, RT, 40, 50, 60, 70 and 80 °C, which was maintained constant throughout the process. The fiber-optic probe was placed inside the RF solution by making a 20 mm opening on the lid of the reaction container (Fig. 1). The UV-vis spectra during the gelation process were recorded at elevated temperatures without stirring. The total volume of the RF solution was fixed as 41 ± 0.1 mL in order to completely cover the optical path length of 10 mm. The volume was calculated by combining the reactant volume (formaldehyde and water) and measured using a measuring cylinder before transferring into the reaction container. The visual progress and the color changes during the sol–gel process are depicted in Fig. 2. The RF solution appeared initially transparent, and turned to different colors with respect to the gelation temperatures over time. The solution turned from transparent to light yellow, light brownish and dark brownish red colors and then changed to turbid appearance followed by gel formation. The wet gel monolith appeared as yellowish brown in color. The direct quantitative link for color changes is not provided with the absorbance values, as the formation of RF polymer cluster is complex. The turbid
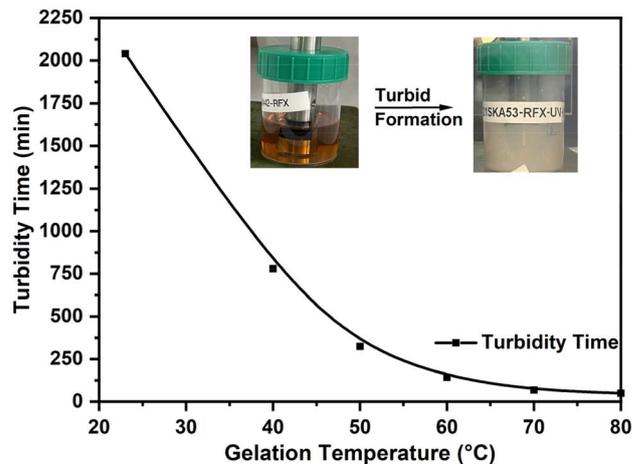
formation during the course of the reaction resulted from the formation of structures with a size relatable to the visible light wavelength.[31,32] The absorption spectrum was recorded *in situ* during the gelation process with different time intervals until turbidity appeared. The time of turbid formation with respect to different gelation temperatures showed a decreasing trend with the increase in gelation temperatures (Fig. 3). The turbidity time is an indication of the physical manifestation of the gelation (*i.e.*, particle formation and aggregation with sizes exceeding visible wavelength) rather than a direct only measure of the chemical reaction kinetics of the system.

3. Results and discussion

3.1. Approach of the study

As mentioned in Section 2.3, the UV-vis spectra of the reaction mixture were measured after step-wise addition of the reactants and stirring. The initial pH of the RF solution was noted down after 30 min of stirring, and the UV-vis spectrum was also recorded. Then, the mixture was placed inside the preheated oven at different gelation temperatures, which was defined as the beginning of the gelation process (0 min). The raw spectrum (absolute absorbance) was subtracted from the water spectrum to obtain the absorbance spectra of the reactant mixtures (corrected absorbance), as depicted in Fig. 4, S1 and S2.†

The UV-vis spectra of RF mixtures in the expanded region are shown in Fig. 5, and the unsaturated spectra of the same are
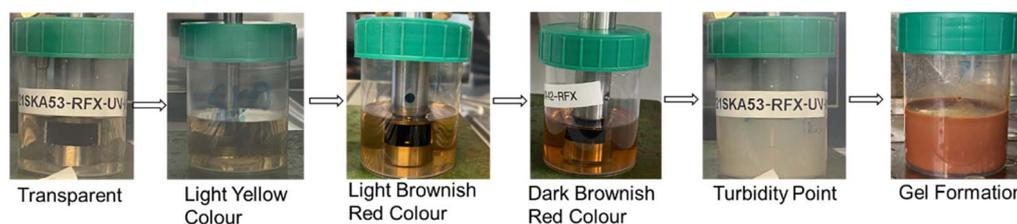

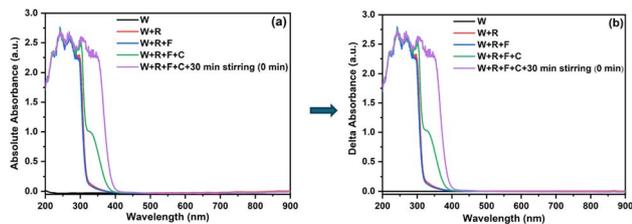Fig. 2 Progress in the color change during the RF gelation process.

Fig. 4 UV-vis spectra of reactant mixtures: (a) before and (b) after water spectra subtraction.

Fig. 6 UV-vis spectra of RF mixtures at 0 and 60 min: (a) before and (b) after 0 min spectra subtraction.

shown in Fig. S3.† The spectrum of resorcinol solution exhibits two absorbance peaks at 273 and 300 nm. The peak at 273 nm is attributed to the aromatic ring present in resorcinol and the peak at 300 nm is assigned to the lone pair of electrons in oxygen atoms.[33] After formaldehyde is added to the mixture, two more absorbance bands are observed at 242 and 280 nm due to n–π and π–π* transitions, respectively.[34] The peak at 283 nm showed an overlapping peak from the sodium carbonate catalyst (Fig. S2†). The short peak observed at 340 nm after mixing all the reactants is assigned to the absorbance of the derivatives of resorcinol formed without heating during the RF solution preparation stage, which are not considered for the evaluation within this work. The spectra were recorded and considered for evaluation at 0 min after placing the reaction container together with a UV-vis probe inside a preheated oven at elevated temperatures.

Fig. 6 represents the UV-vis spectra of the RF mixture, which were recorded at 0 and 60 min at 60 °C. The absolute spectrum at 0 min (Fig. 6a) shows a peak at 340 nm that indicates resorcinol derivatives. The peak at 340 nm is shifted to a higher wavelength of 400 nm and a new less intense peak is formed at around 500 nm after 60 min at 60 °C. The peak ranging between 340 and 400 nm results from the conjugated benzene rings present in the different derivatives of resorcinol (substituted resorcinol or hydroxymethyl derivatives with mono-, di- and tri-substituted resorcinol)[35] formed. Very recently, the presence of
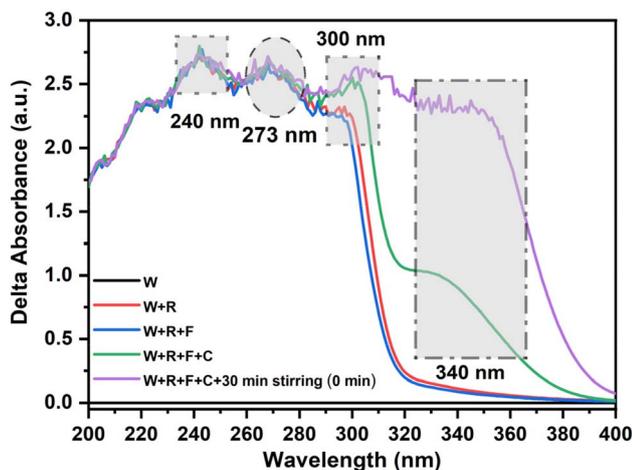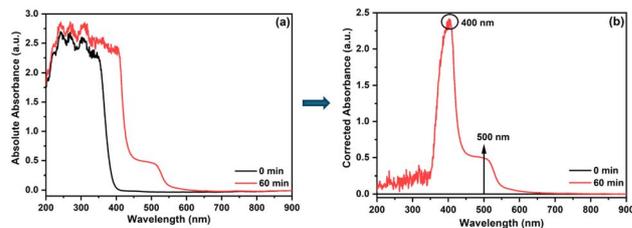
conjugated rings in RF resins has been evidenced by Shiraishi et al.[36] RF resins produced under high-temperature and high-pressure hydrothermal conditions result in large numbers of quinonoid forms of resorcinol, which act as electron acceptors. The electron acceptors are π-conjugated with inherent benzenoid forms of resorcinol. The second less intense absorption peak at around 500 nm results from the O-quinone methide intermediate formed during the reaction. Mulik et al.[21] observed a strong absorption peak at 543 nm, indicating the O-quinone methide intermediate developed during the HCl-catalysed RF gel formation, which was well supported by the development of strong red color.[21] They reported that the brick red color of the aerogel results from the configurationally locked O-quinone derivative. Furthermore, they visually observed that RF aerogels produced with an R/F ratio of 0.1 were much lighter in color than the gels with an R/F ratio of 0.5 due to the difference in the amount of O-quinone methide formed. It clearly confirms that the nature and intensity of the color are dependent on the amount of O-quinone intermediate formed.

3.2. In-line monitoring of RF gelation at various gelation temperatures in real time

3.2.1. Gelation at RT.
The raw (representative 3D spectrum in Fig. S4†) and background subtracted (using 0 min spectra) spectra of the RF solution measured at RT during the gelation are presented in Fig. 7 and S5.† Table 1 represents the turbidity time and absorbance value time trends for the first and second peaks. The absorption spectrum of RF at RT was recorded until the turbid point (∼2040 min) and the peak at 340 nm appears from the beginning of the gelation. As the gelation progresses, first absorbance maximum is increased and red shifted towards a higher wavelength (400 nm). The red shift is an indication of growing conjugation in the RF polymer network.[24] A similar kind of red shift was shown by colloidal C_{60} particles dispersed in water compared to free C_{60}.[37] The appearance of two broad absorption peaks in the wavelength range of 250–750 nm is the characteristic of aqueous colloidal C60 particles yellow in color (RF solution shows yellow color). The two strong absorption peaks of an aqueous solution of C_{60} particles with different sizes (110 and 230 nm) are red shifted with respect to the increase in particle size, which is proportional to the size of the particles. As shown in Fig. 7, the increased absorption and red shift of the peak at 340 nm can be correlated with the following: a change in the color of RF solution (colorless to orange red, Fig. 2), growing π-conjugations,[36] increase in primary particle size and

Fig. 5 Expanded regions (200–400 nm) of the UV-vis spectra of the reactant mixtures.
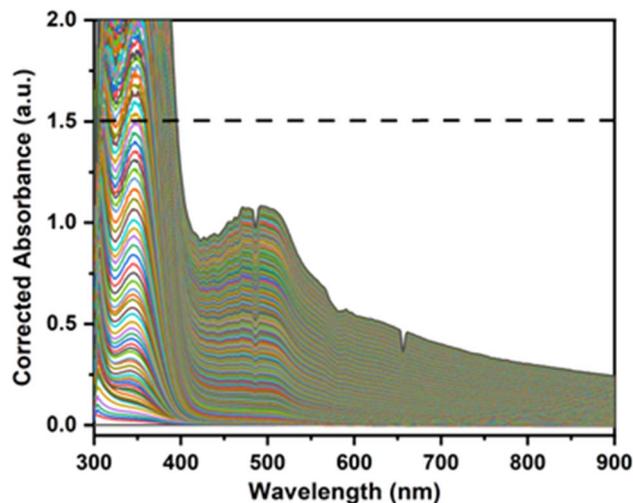
Fig. 7 UV-vis spectrum of the RF mixture during gelation at RT after background subtraction.

viscosity[38] and growth or aggregation of primary particles or clusters[35] as the polycondensation reaction proceeds.

The peak at around 500 nm related to *O*-quinone methide requires a minimum induction time (discussed later) to appear during the gelation process (Fig. 7). The reaction chemistry of the RF polymer is quite similar to the PF polymer. According to Li *et al.*,[39] the formation of *O*-quinone methide is the rate-determining step during the condensation reaction of the PF. The reactive intermediates at the molecular level are important in determining the rate of the condensation reaction.[40] DFT calculations of the base-catalysed PF reaction confirmed that the mechanism involved not only the formation of *O*-quinone methide but also the formation of *P*-quinone methide. The formation of *P*-quinone methide is much faster than *O*-quinone methide, which is evidenced from the potential energies of *O*-quinone methide and *P*-quinone methide as 108.0 and 83.6 kJ mol^{-1}, respectively. The latter must overcome 24.4 kJ mol^{-1} less energy barrier than the former.[39] Hence, RF condensation has a much high energy barrier and requires more energy and more time for the formation of intermediates (~200 min) at RT. The increase in the absorption value with regard to the first and second absorption maximum is discussed in detail below.
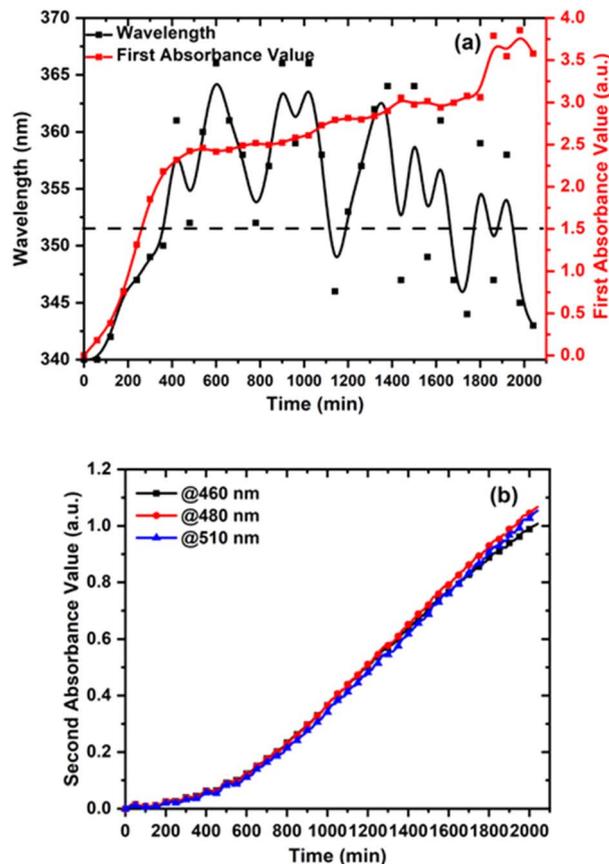

Fig. 8 Kinetic monitoring of the UV-vis absorbance of the RF solution at RT: (a) first absorbance value and its respective wavelength maximum *versus* time and (b) second absorbance value *versus* time with respect to three different wavelengths.

The kinetic absorbance values of RF solution at RT with respect to the first and second absorption peaks are depicted in Fig. 8. In Fig. 8a, the absorbance values until 4 is presented. However, the discussions are limited to absorbance values of ≤1.5 considering the deviation of the non-linear behavior of the calibration curve according to Beer–Lambert's law. A strategic cut-off line is placed at an absorbance value of 1.5 in all the UV-vis spectra in order to meticulously show that the evaluation and discussion are limited to an absorbance value ≤1.5. The first absorption peak attains the absorption value of 1 at

Table 1 Turbidity time and absorption time trend for the first and second peaks

Sample codes	Gelation temperature (°C)	Turbidity time (min)	First absorbance peak value time (min)		Second absorbance peak induction time (min)
			1	1.5	
S1	RT	2040	200	260	200
S2	40	780	45	55	100
S3	50	325	35	41	75
S4	60	142	25	29	35
S5	70	68	16	17	20
S6	80	49	14	15	15

200 min and exceeds 1.5 at 260 min. The absorptions between 250 and 2040 min show an increased absorbance value between 1.5 and 4 (spectra above 2 is not presented). The spectrum cannot be measured after the turbid point which means that the gelation at RT requires a minimum of 2040 min in order to result in the formation of structures with a size in the visible region. It evidenced the slower reaction (or gelation) kinetics of RF solution at RT with a longer gelation time.[41] Li *et al.*[41] reported that the low-temperature growth of low-concentrated RF solutions (R/C = 100, F/R = 2 with densities of 100 and 200 mg cm^{-3} (varied R/W ratio)) adopts the nucleation-dominant growth model of network, which requires longer nucleation and gelation time. However, high-concentration RF solutions (densities of 300, 400 and 500 mg cm^{-3} (varied R/W ratio)) adopt the diffusion-dominant growth model. It has also been reported that the viscoelastic component of RF reactants at the gel point decreased with the increase in gelation temperature. The viscoelastic moduli of RF solution (density of 200 mg cm^{-3}) at 30 and 60 °C were found to be 162 and 1.9 Pa, respectively. The higher viscoelastic modulus at a lower temperature supports the adaptation of the growth-dominant model during a longer gelation process. Overall, the gelation temperature shows great influence on the growth mechanism of the RF particles. The growth mechanism is correlated with respect to the absorbance changes and turbidity point at a lower gelation temperature. The appearance of second absorbance requires an induction time of 200 min to appear and exhibit a steady-state behavior. Further, it has a linear behavior until the turbid point.

3.2.2. Gelation at 40 °C. The in-line UV-vis absorption spectrum of RF solution was recorded at 40 °C until the appearance of turbidity at 780 min in real time. The raw and background-corrected spectra at 40 °C are depicted in Fig. 9 and S6.† The increase in gelation temperature from RT to 40 °C drastically decreased the turbidity time from 2040 to 780 min, which evidenced the increase in speed and rate of the reaction. Among several process variables influencing the textural and

structural properties of the gel formed, the gelation temperature has a great impact on the overall process cost.[42] The decrease in the turbidity time is directly related to the formation of particle structures at a faster rate, which adopts the diffusion-dominant model proposed by Li *et al.*[41] for the particle network growth and well supported by the decrease in viscoelastic strength at high temperatures. This phenomenon is quite relevant for the understanding of the decrease in turbidity time with respect to the increase in gelation temperatures in our study. The UV-vis kinetic monitoring of first and second absorbance maxima in correlation with their respective wavelengths is presented in Fig. 10. The first absorbance value exceeds a maximum of 1 and 1.5 at gelation times greater than 45 and 55 min, respectively. The second absorbance value with respect to three different wavelengths exhibits a steady-state behavior up to 100 min and shows a linear trend after 100 min until turbidity appeared.

3.2.3. Gelation at 50 °C. The absolute and corrected spectra of the RF solution at 50 °C were measured up to 325 min, and are presented in Fig. 11 and S7.† The gelation temperature is doubled from room temperature (∼23 °C) to 50 °C, which
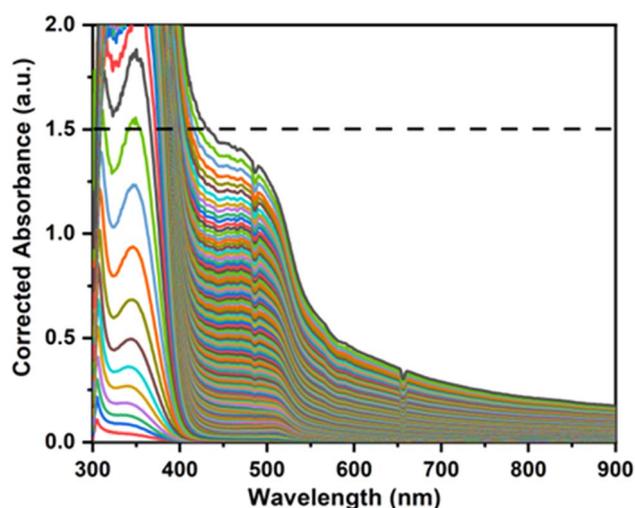

Fig. 9 UV-vis spectrum of the RF mixture during gelation at 40 °C after background subtraction.
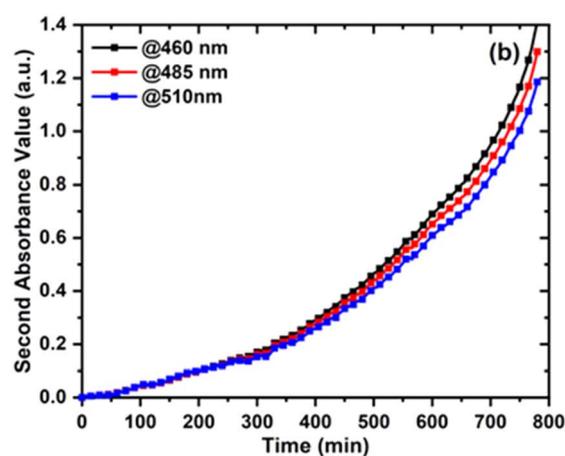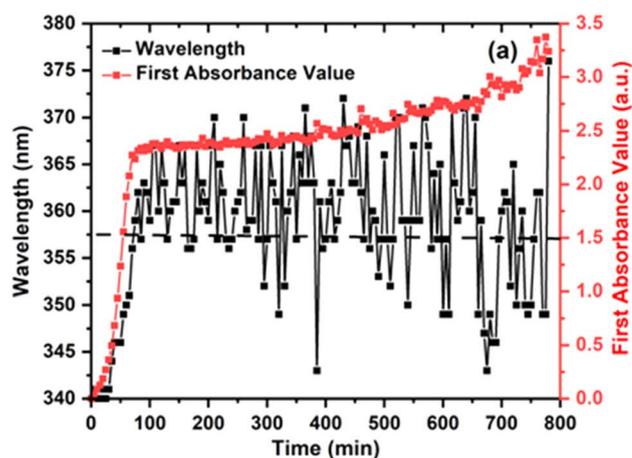
Fig. 10 Kinetic monitoring of the UV-vis absorbance of the RF solution at 40 °C: (a) first absorbance value and its respective wavelength maximum *versus* time and (b) second absorbance value *versus* time with respect to three different wavelengths.
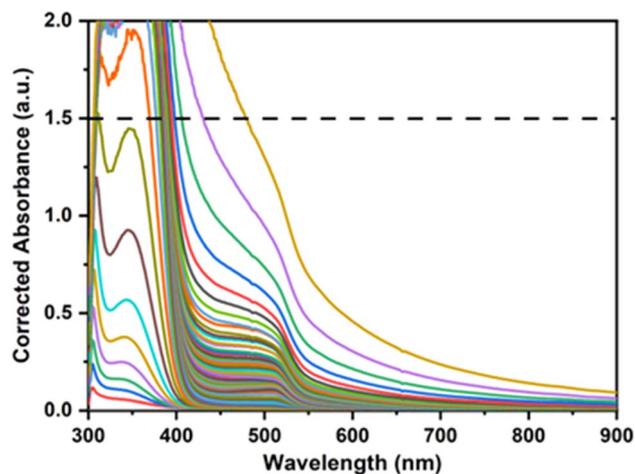
Fig. 11 UV-vis spectrum of the RF mixture during gelation at 50 °C after background subtraction.

resulted in a 6.5-fold decrease in turbidity time from 2040 to 325 min. The appearance of turbidity is because of the formation of particles, which is in good correlation with the DLS investigations of RF solutions at 55 °C reported by Gaca *et al.*[3] They observed that the mean hydrodynamic radius of primary RF clusters formed during the initial stage is independent of the R/C ratio but dependent on the gelation temperatures. The hydrodynamic radius of the hydrated resorcinol molecule was found to be 0.4 nm. The size of the primary clusters increased from 1.5 to 3.5 nm at 10 and 50 min, respectively, at 55 °C.[3] These primary clusters led to aggregation and subsequent gelation over time. We observed a strong violent fluctuation of the absorbance at the turbid point due to large particle formation, which is the limitation of UV-vis technique to follow the absorbance changes beyond turbidity. Li *et al.*[41] investigated the particle growth kinetics of RF using time-resolved DLS (TR-DLS) at 50 °C. They observed violent fluctuation in the scattered intensity, $I(t)$, after the gelation threshold because of the non-uniform and multiple scattering of gel particles. Tamon *et al.*[43] has also reported that doubling the gelation temperature from 25 to 50 °C did not influence the mesoporous structure of the aerogels. However, the increase in gelation temperature can thermodynamically speed up the formation of more clusters and shorten the turbidity and gelation time. The increase in absorbance value with respect to first and second absorbance maxima is presented in Fig. 12. The first absorbance value at 50 °C exceeds absorption maxima of 1 and 1.5 at 35 and 41 min, respectively. The second absorbance value exhibits a steady and linear behavior until 75 min and increases rapidly up to 300 min and attains maximum at the turbid point. This sharp increase in absorbance value is in good correlation with the formation of large clusters and further aggregation, which leads to turbidity.

3.2.4. Gelation at 60 °C. The absorbance changes during RF gelation were monitored at 60 °C, and their respective spectra are presented in Fig. 13 and S8.† The increase in gelation temperature from 50 to 60 °C further decreased the turbidity time from 325 to 142 min. It is clearly evident that the
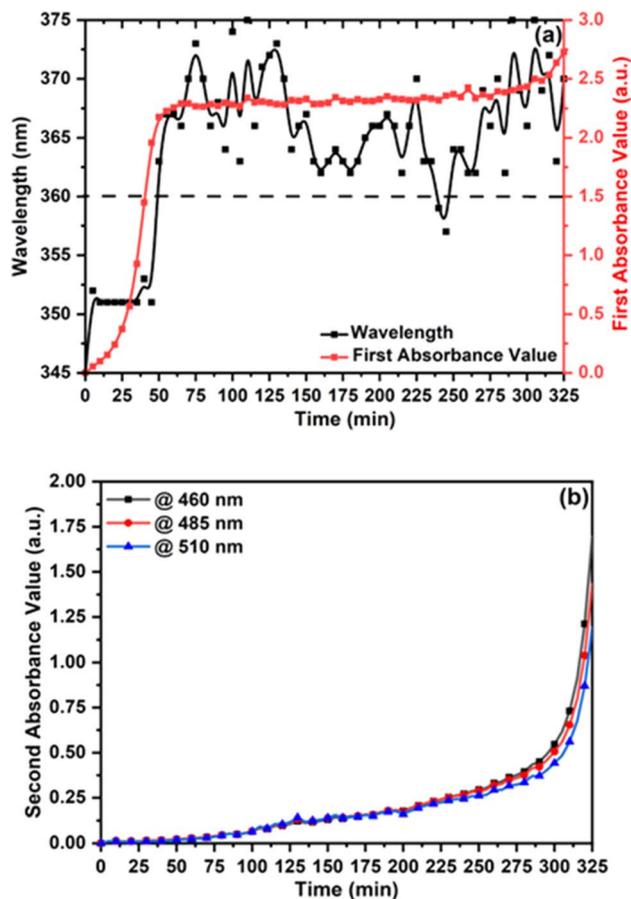

Fig. 12 Kinetic monitoring of the UV-vis absorbance of the RF solution at 50 °C: (a) first absorbance value and its respective wavelength maximum *versus* time and (b) second absorbance value *versus* time with respect to three different wavelengths.
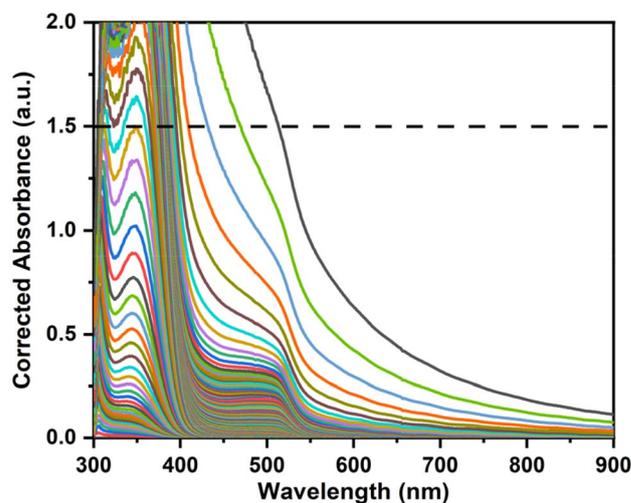

Fig. 13 UV-vis spectrum of the RF mixture during gelation at 60 °C after background subtraction.

turbidity time is reduced by a factor of 2.6 times at 60 °C in comparison to 50 °C. The gelation temperature >55 °C is a key factor in initiating the growth of RF clusters once the reactant

mixture attains 55 °C. This is in good agreement with the decreased turbidity time with regard to the increase in gelation temperature by more than 5 °C after attaining the minimum threshold temperature of 55 °C for water as a solvent, as reported by Prostredný et al.[42] It can be clearly seen that the gelation temperature >55 °C is an important factor to achieve faster RF particle cluster growth. The particle growth mechanism of RF solutions of different R/C ratios by DLS has been well studied and reported by Taylor et al.[35] at a temperature >55 °C. They also observed that irrespective of the R/C ratios, hydrodynamic radii were less than 1 nm and do not grow for a certain period of time. The hydrodynamic radius of the hydrated resorcinol molecule is 0.4 nm.[3] The delay in particle growth was correlated with the time taken for achieving the gelation temperature of 55 °C. Taylor et al.[24] recommended that preheating of the initial reactant solution to 55 °C can eliminate such a delay of particle growth. In our investigation, we clearly observed the decrease in turbidity time by factors of 2.6, 6.5 and 14.5 for 40, 50 and 60 °C, respectively, in comparison to RT. The

kinetic monitoring of first and second absorbance maxima with respect to wavelengths is presented in Fig. 14. The first absorbance value exceeds 1 and 1.5 at a gelation time greater than 25 and 29 min, respectively. The second absorbance value with respect to the O-quinone methide derivative at three different wavelengths exhibited steady behavior until 35 min and increased rapidly up to 120 min and reached the maximum close to the turbid point. The curve (Fig. 14b) seems to exhibit an S-shape and is quite flat at the early stages of gelation up to 35 min, which is a kind of an 'induction' time (minimum time required to form an intermediate). The 'induction' time of 35 min is the time required to reach first absorbance maximum of 2 and the appearance of second absorbance peak. As discussed in Section 3.1, first and second absorbance peaks correspond to derivatives of resorcinol and the formation and interlocking of O-quinone methide and/or their spiro derivatives, respectively. This hypothesis was proven by Mulik et al.[21] by decolorizing the HCl-catalysed RF aerogel by immersing it in a NaBH$_4$ solution and redeveloping the red color by washing and exposing them to air. After the induction period, the second absorbance value starts to evolve and reaches a high value near the turbid point.

3.2.5. Gelation at 70 °C. The absorbance changes and kinetic information of RF at 70 °C were monitored, and are presented in Fig. 15, S9 and S16.† The increase in gelation temperature from 60 to 70 °C caused a double-fold decrease in the turbidity time from 142 to 68 min. Job et al.[44] reported the influence of synthesis condition (R/C ratio) and temperature on gelation time observed by rheology and/or visually. The gelation temperature is the driving force to speed up the transition from sol to gel that leads to the development of inter-connected structures at gelation time via turbidity. The inter-connections between particles were formed either by weak and/or strong interactions for reversible and/or permanent gels.[44,45] As per our investigation, the absorbance changes associated with chemical reactions during the gelation greatly depend on the
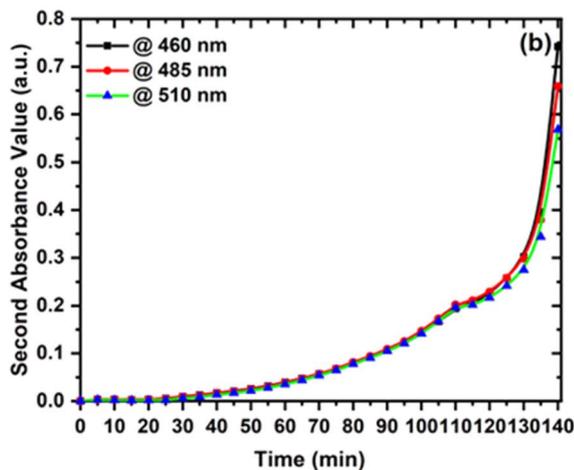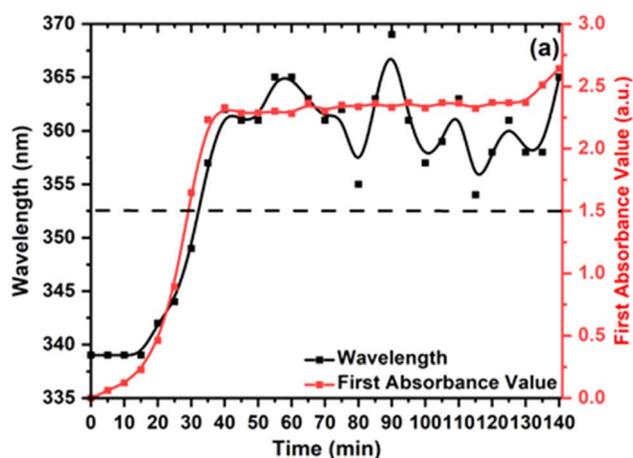

Fig. 14 Kinetic monitoring of the UV-vis absorbance of the RF solution at 60 °C: (a) first absorbance value and its respective wavelength maximum versus time and (b) second absorbance value versus time with respect to three different wavelengths.
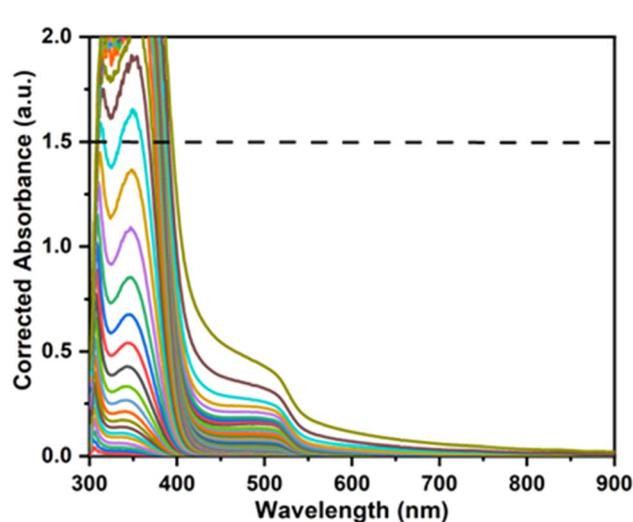

Fig. 15 UV-vis spectrum of the RF mixture during gelation at 70 °C after background subtraction.

temperature, which also influences the viscosity of the system.[46] It has been observed that the rise in viscosity directly depends on the temperature. The initial increase in viscosity is attributed to the polymerization and particle generation, which remains constant for a particular period of time. During this time interval, particles collide with each other due to Brownian motion and aggregate *via* reactions of the surface functional groups. The second increase in viscosity was observed with linearity with respect to gelation time. They also observed that the increase in gelation temperatures from 60 to 70 °C and further to 80 °C resulted in a shorter gelation time, which can be correlated with the faster particle aggregation because of the greater Brownian motion. We strongly believe that a similar kind of phenomena is attributed to the decreased turbidity time of 68 min at 70 °C. The monitoring of changes associated with the first and second absorbance values with respect to time is presented in Fig. 16. The first absorbance exceeds the values of 1 and 1.5 at short time-intervals of 16 and 17 min, respectively (Fig. 16a). The second absorbance values (Fig. 16b) show a linear increasing trend until 20 min, increase rapidly up to 60 min and attain maximum close to the turbidity time.
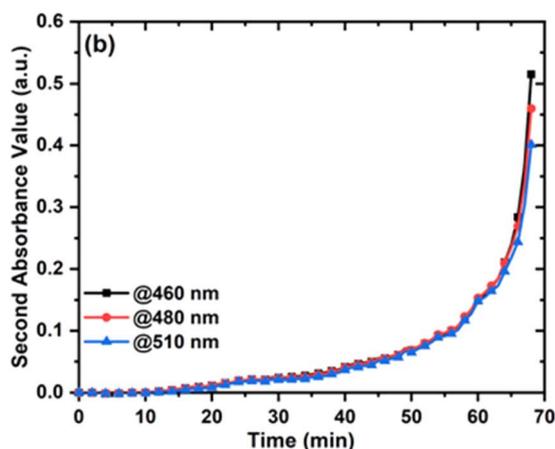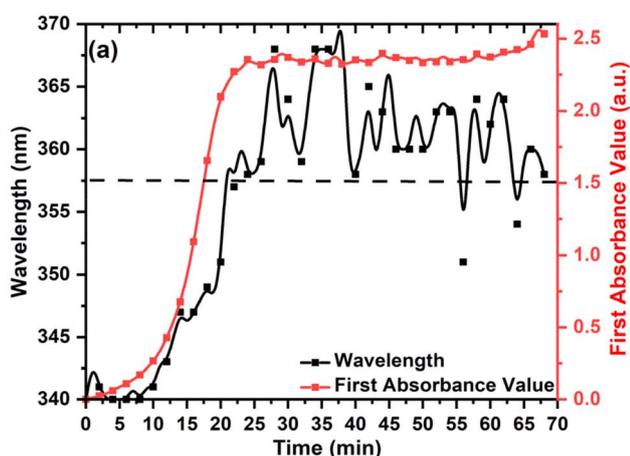

Fig. 16 Kinetic monitoring of UV-vis absorbance of the RF solution at 70 °C: (a) first absorbance value and its respective wavelength maximum *versus* time and (b) second absorbance value *versus* time with respect to three different wavelengths.

3.2.6. Gelation at 80 °C. In Fig. 17 and S10,† the absorption changes of RF at 80 °C before and after background subtraction are presented. The increase in gelation temperature from 70 to 80 °C further decreased the turbidity time from 68 to 49 min. The increment of 10 °C caused a decrease in turbidity time by a factor of 1.4, as expected. Gaca *et al.*[14] performed time-resolved DLS experiments of the RF solution at 55 and 80 °C after quenching them at 20 °C. They reported that both temperatures have the same kind of autocorrelation functions, exhibiting transition from monodisperse population of primary clusters initially through polydisperse collection of aggregated clusters to a gel network of interconnected clusters. They also noticed that the aggregation stage was observed only after 50 min at 55 °C, whereas it was just 10 min at 80 °C. The decrease in the aggregation time at a higher temperature greatly supports our claim of decrease in turbidity time to 49 min at 80 °C. The turbidity times at RT and 80 °C clearly indicate the strong dependence of chemical or gelation kinetics of the RF system on temperature. As mentioned earlier, resorcinol reacts with formaldehyde to yield hydroxymethyl resorcinol, which forms the polymer. The degree of polymerization (DP), *i.e.*, DP = DP(t), and the volume fraction of the polymers, $\phi(t)$, are time dependent.[47] Ratke and Gurikov[47] pointed out that the RF system may exhibit a miscibility gap similar to the one present in the phase diagram of the polymer and solvent system described by the Flory–Huggins (FH) model.[48] They also pointed out that the RF system exhibits a lower critical solution temperature. We observed that the RF solution maintained at 60 °C is present without gelation when it is suddenly transferred to a fridge (Fig. S11 and S12†). This phenomenon is never possible if the system exhibits upper critical solution temperature. It has been proposed that during the gelation process under heating, the miscibility gap develops and miscibility point shifts towards a two-phase region. In two-phase regions, polymer-rich droplets start to appear and their volume of fraction and size will change with respect to time. Further, the solution starts to turn into
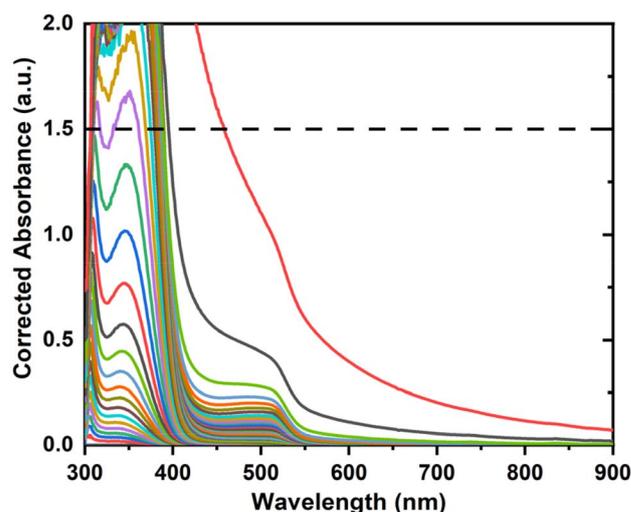

Fig. 17 UV-vis spectrum of the RF mixture during gelation at 80 °C after background subtraction.
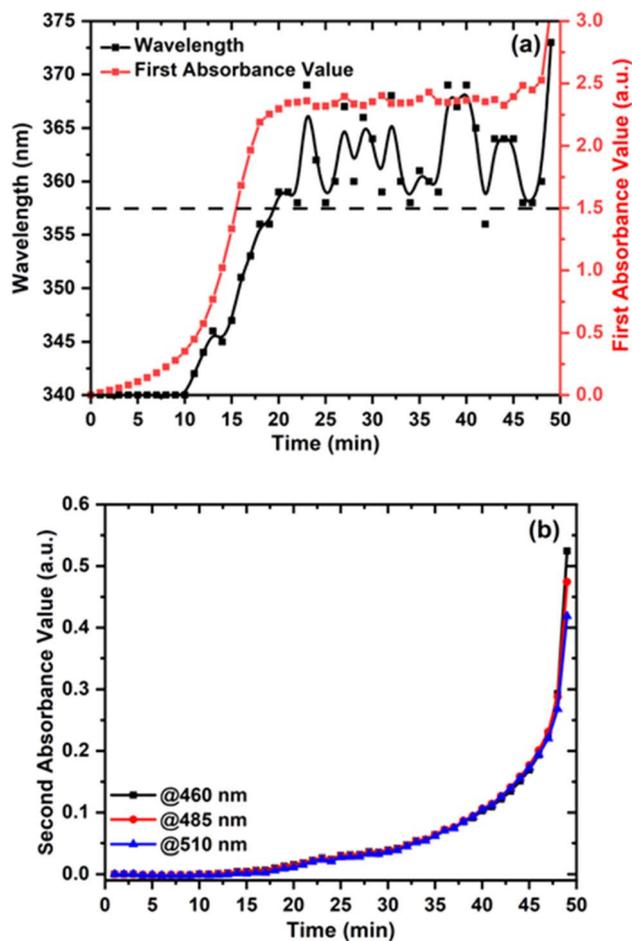
Fig. 18 Kinetic monitoring of UV-vis absorbance of the RF solution at 80 °C: (a) first absorbance maxima and its respective wavelength maximum *versus* time and (b) second absorbance maxima *versus* time with respect to three different wavelengths.

a suspension (turbid) of droplets in a polymer-depleted solvent and transform into a wet gel particle.[47] The solid-like gel polymeric network particles are formed in a liquid matrix with varying degrees of polymerization at the end of phase separation.

The changes in absorbance value with respect to time and wavelength for the first and second absorbance maxima are presented in Fig. 18a and b. The first absorbance exceeds the value of 1 and 2 after 14 and 15 min. The second absorbance values at different wavelengths show a linear trend until 15 min and rapidly increase until 45 min. It reaches a maximum value near to the turbid point of 49 min. The curve exhibits an increasing trend of assumed 'S'-type shape.

4. Summary

The current study presents the kinetic monitoring of gelation of RF solutions using real-time UV-vis spectroscopy by in-line measurements through a fiber-optic probe. The two characteristic absorbances of RF solutions were monitored at different gelation temperatures until the appearance of visible turbidity.

The first absorbance peak ranging from 340 to 400 nm caused by the conjugated benzene ring started to appear immediately, whereas the second absorbance peak ranging from 460 to 510 nm related to *O*-quinone methide intermediate required a minimum induction time due to its high energy barrier (108.0 kJ mol^{-1}).[39] The gelation at RT required a longer time for the attainment of absorbance value of 1 (200 min) and for the appearance of turbidity (2040 min). The increase in gelation temperature to 40 °C greatly influenced the speed and rate of the reaction, which is clearly evident from the decrease of turbidity time from 2040 to 780 min. The decrease in turbidity time is directly correlated with the fast formation of particle structures within a short time of 780 min. Moreover, the attainment of an absorbance value of 1 required only 45 min (for 40 °C) in comparison to RT (200 min). In the case of 50 °C, a 6.5-fold decrease in turbidity time from 2040 to 325 min was observed. This is in accordance with the growth of primary clusters at 55 °C, as reported by Gaca *et al.*[3] The fast growth of primary clusters led to faster aggregation and gelation at 55 °C with a faster turbidity time of 325 min. The first absorbance value reached a maximum of 1 within a short time of 35 min. The increase in gelation temperature to 60 °C further decreased the turbidity time by a factor of 2.6 (325 to 142 min for 50 to 60 °C). The first absorbance maximum reached a value of 1 at 25 min and the appearance of the second absorbance peak at around 500 nm required an 'induction time' of 30 min, where the first absorbance maxima reached a value of 2. The further increase in gelation temperature to 70 °C resulted in a 2-fold decrease in turbidity time. The increase in gelation temperature increases the Brownian motion of the particles, which leads to the faster aggregation of the particles, thereby decreasing the turbidity and gelation time. The first absorbance value reached a maximum value of 1.5 at a short time-interval of 17 min. A further increase in gelation temperature to 80 °C decreased the turbidity time to 49 min. The increase in gelation temperature has a direct influence on the transition of monodisperse population of primary clusters through polydisperse collection of aggregated clusters into a gel network. This phenomenon was clearly reflected in the faster turbidity time and rapid attainment of the first absorbance value of 1.5 within 15 min at 80 °C.

This type of UV-vis kinetic investigation of RF solutions at different gelation temperatures by monitoring absorbance changes will provide an important insight into the early-stage gelation kinetics and mechanisms of RF. This study should not be limited to only UV-vis, but it should be coupled with other techniques such as DLS or SEM to understand the complete gelation kinetics and mechanisms and further the influence on the microstructure and other properties of RF aerogels. In additions, investigations on costs should be considered in order to make the sol–gel process of RF less time and energy intensive.

5. Conclusions

The real-time monitoring of the gelation process of resorcinol–formaldehyde solutions by in-line UV-vis spectroscopy using a fiber-optic probe was studied at different gelation temperatures. The changes in the two characteristic absorption peaks at

around 340–400 and 500 nm were followed during the sol–gel transition. The turbidity time of RF solution was 2040 min at RT and decreased to 49 min at 80 °C. The first absorbance peak appeared at the beginning of the gelation reaction and the second absorbance peak evolved after a certain period of induction time to form *O*-quinone methide. The increase in the second absorbance peak was steady and linear in the cases of RT and 40 °C, whereas the trend at temperatures ≥50 °C was a kind of 'S'-type curve. Further investigations are in progress to understand the very early stages of reaction kinetics and quantify the species formed by changing the recipe and other parameters and also the reaction rate and rate constants.

Data availability

The data supporting this article have been included as part of the ESI.†

Author contributions

Conceptualization, methodology, validation, writing – original draft, writing – review & editing, visualization: S. M. K. M.; methodology, validation, writing – review & editing: K. M.; project administration, writing – review & editing: C. H., project administration, writing – review & editing: M. S.; project administration, writing – review & editing, supervision: B. M.

Conflicts of interest

There are no conflicts to declare.

Acknowledgements

References

1 R. Pekala and F. Kong, *J. Phys. Colloq.*, 1989, **50**, 33–40.
2 S. M. Kamal Mohamed, C. Heinrich and B. Milow, *Polymers*, 2021, **13**, 2409.
3 K. Z. Gaca and J. Sefcik, *J. Colloid Interface Sci.*, 2013, **406**, 51–59.
4 J. Laskowski, B. Milow and L. Ratke, *Microporous Mesoporous Mater.*, 2014, **197**, 308–315.
5 E. G. Calvo, J. A. Menéndez and A. Arenillas, *J. Non-Cryst. Solids*, 2016, **452**, 286–290.
6 A. M. ElKhatat and S. A. Al-Muhtaseb, *Adv. Mater.*, 2011, **23**, 2887–2903.
7 I. D. Alonso-Buenaposada, N. Rey-Raap, E. G. Calvo, J. A. Menéndez and A. Arenillas, *J. Sol-Gel Sci. Technol.*, 2017, **84**, 60–69.
8 N. Rey-Raap, J. Angel Menéndez and A. Arenillas, *Carbon*, 2014, **78**, 490–499.
9 R. W. Pekala and D. W. Schaefer, *Macromolecules*, 1993, **26**, 5487–5493.
10 T. Yamamoto, T. Yoshida, T. Suzuki, S. R. Mukai and H. Tamon, *J. Colloid Interface Sci.*, 2002, **245**, 391–396.
11 D. W. Schaefer, R. Pekala and G. Beaucage, *J. Non-Cryst. Solids*, 1995, **186**, 159–167.
12 R. B. Durairaj, *Resorcinol: Chemistry, Technology and Applications*, Springer Science & Business Media, 2005.
13 C. J. Gommes and A. P. Roberts, *Phys. Rev. E:Stat., Nonlinear, Soft Matter Phys.*, 2008, **77**, 041409.
14 K. Z. Gaca, J. A. Parkinson and J. Sefcik, *Polymer*, 2017, **110**, 62–73.
15 M. Kéri, B. Nagy, K. László and I. Bányai, *Microporous Mesoporous Mater.*, 2021, **317**, 110988.
16 K. Z. Gaca-Zając, B. R. Smith, A. Nordon, A. J. Fletcher, K. Johnston and J. Sefcik, *Vib. Spectrosc.*, 2018, **97**, 44–54.
17 J. Monni, P. Niemelä, L. Alvila and T. T. Pakkanen, *Polymer*, 2008, **49**, 3865–3874.
18 R. Tannert, M. Schwan and L. Ratke, *J. Supercrit. Fluids*, 2015, **106**, 57–61.
19 S. Mulik and C. Sotiriou-Leventis, in *Aerogels Handbook*, Springer, 2011, pp. 215–234.
20 A. Pizzi and C. C. Ibeh, in *Handbook of Thermoset Plastics*, ed. H. Dodiuk and S. H. Goodman, William Andrew Publishing, Boston, 3rd edn, 2014, pp. 13–44, DOI: **10.1016/B978-1-4557-3107-7.00002-6**.
21 S. Mulik, C. Sotiriou-Leventis and N. Leventis, *Chem. Mater.*, 2007, **19**, 6138–6144.
22 M. Engeldinger, *Compt. Rend.*, 1936, **202**, 1854.
23 P. J. Stedry, *Ind. Eng. Chem.*, 1951, **43**, 2372–2375.
24 S. J. Taylor, PhD Doctoral thesis, University of Strathclyde, 2014.
25 T. H. A. Berg, N. Ottosen, F. van den Berg and R. Ipsen, *LWT–Food Sci. Technol.*, 2017, **75**, 164–170.
26 W. Schlindwein, M. Bezerra, J. Almeida, A. Berghaus, M. Owen and G. Muirhead, *Pharmaceutics*, 2018, **10**, 166.
27 F. Gao, L. Wang, H. Zhang and J. Wang, *Chem. Eng. J. Adv.*, 2020, **4**, 100058.
28 Y. Y. Sun Qingqing, W. Shuai, L. Panyi, B. Lin and L. Huabing, *R. Soc. Open Sci.*, 2020, 7, 200461.
29 R. S. Lankone, A. R. Deline, M. Barclay and D. H. Fairbrother, *Talanta*, 2020, **218**, 121148.
30 H. Terraschke, M. Rothe and P. Lindenberg, *Rev. Anal. Chem.*, 2018, **37**, 20170003.
31 T. Tanaka, *Sci. Am.*, 1981, **244**, 124–138.
32 C. J. Gommes, N. Job, J.-P. Pirard, S. Blacher and B. Goderis, *J. Appl. Crystallogr.*, 2008, **41**, 663–668.
33 S. M. Attia, M. S. Abdelfatah and M. M. Mossad, *J. Phys.: Conf. Ser.*, 2017, **869**, 012036.
34 M. R. Leonardo, L. A. B. da Silva, M. T. Filho and R. S. da Silva, *Oral Surg. Oral Med. Oral Pathol. Oral Radiol. Endod.*, 1999, **88**, 221–225.

35 S. J. Taylor, M. D. Haw, J. Sefcik and A. J. Fletcher, *Langmuir*, 2014, **30**, 10231–10240.

36 Y. Shiraishi, T. Takii, T. Hagi, S. Mori, Y. Kofuji, Y. Kitagawa, S. Tanaka, S. Ichikawa and T. Hirai, *Nat. Mater.*, 2019, **18**, 985–993.

37 H. Kato, A. Nakamura, K. Takahashi and S. Kinugasa, *Phys. Chem. Chem. Phys.*, 2009, **11**, 4946–4948.

38 E. Kinnertová, V. Slovák, R. Maršálek and M. Mucha, *Gels*, 2022, **8**, 8.

39 T. Li, M. Cao, J. Liang, X. Xie and G. Du, *Polymers*, 2017, **9**, 45.

40 T. Li, M. Cao, J. Liang, X. Xie and G. Du, *Polymers*, 2017, **9**, 426.

41 J. Li, X. Yang, L. Yuan, Z. Li, Y. Zeng and H. Shen, *Colloids Surf., A*, 2022, **648**, 129300.

42 M. Prostredný, M. G. M. Abduljalil, P. A. Mulheran and A. J. Fletcher, *Gels*, 2018, **4**, 36.

43 H. Tamon and H. Ishizaka, *J. Colloid Interface Sci.*, 2000, **223**, 305–307.

44 N. Job, F. Panariello, M. Crine, J.-P. Pirard and A. Léonard, *Colloids Surf., A*, 2007, **293**, 224–228.

45 A. Ponton, S. Barboux-Doeuff and C. Sanchez, *J. Non-Cryst. Solids*, 2005, **351**, 45–53.

46 S. A. Letts, S. R. Buckley, F.-M. Kong, E. F. Lindsay and M. L. Sattler, *MRS Online Proc. Libr.*, 1989, **177**, 275–279.

47 L. Ratke and P. Gurikov, in *The Chemistry and Physics of Aerogels*, Cambridge University Press, Cambridge, 2021, pp. 11–59, DOI: **10.1017/9781108778336.003**.

48 P. Atkins, J. De Paula, and J. Keeler, *Atkins' Physical Chemistry*, Oxford University Press, 11th edn, 2017.